Self-similar bandgap structure and spin-polarized transport in quasiperiodic cascade junctions of ferromagnet and semiconductor

Jia Li, R. L. Zhang,[a)] R. W. Peng,[b)] Xin Wu, De Li, Qing Hu, Yan Qiu, and Mu Wang
National Laboratory of Solid State Microstructures and Department of Physics, Nanjing University, Nanjing 210093, China

(Presented 12 November 2008; received 16 September 2008; accepted 27 November 2008; published online 19 March 2009)

We theoretically investigate spin-dependent transport in quasiperiodic cascade junctions of a ferromagnetic metal (FM) and semiconductor (SC), where FM and SC are arranged in the Fibonacci sequence. It is shown that spin-up and spin-down electrons possess different bandgap structures against the Rashba spin-orbit wave vector. The spin-dependent bandgap structure has the hierarchical characteristic and present self-similarity. Due to the quasiperiodicity, multiple resonant transmissions for spin-up or spin-down electrons can be observed within the bandgap; thereafter, spin polarization has multiple reversals. And it is also found that the electrical conductance can come from one kind of spin electrons around the resonant wave vector. These investigations may provide a unique way to design the devices such as spin filters and spin switches. © *2009 American Institute of Physics*. [DOI: 10.1063/1.3073655]

The discovery of quasicrystals in 1984 has attracted great interest both theoretically and experimentally.[1] The Fibonacci sequence is one of the well-known examples in one-dimensional quasiperiodic systems. It contains two building blocks (A, B) and can be produced by repeating the substitution rules $A \rightarrow AB$ and $B \rightarrow A$. Since Merlin *et al.*[2] reported the first realization of Fibonacci superlattices, much attention has been paid to the exotic wave phenomena of Fibonacci systems in x-ray scattering spectra,[2,3] electronic transmission, and optical transmission spectra.[4] It is found that the self-similarity can be considered as a basic signature of these systems. Compared to the periodic structures, more structural parameters can be tuned in the quasiperiodic designs, thus opening a way to a wide range of technological applications in several different fields.[5]

On the other hand, spin-polarized transport in ballistic quantum systems has recently been discussed. A typical system is the Datta–Das spin field-effect transistor,[6] where ferromagnetic metals (FMs) are used as spin injectors and detectors and are connected to a semiconductor (SC). Relatively high spin injection efficiencies have been achieved in the experiment.[7,8] Quantum spin-valve effect,[9] switching effect, and spin filtering in FM/SC heterostructures have also been reported.[10] It becomes interesting to manipulate the spin-polarized transport by designing various FM/SC junctions. In order to achieve various functional spin-dependent materials and devices, we will study the quasiperiodic cascade junctions of FM and SC because there are more structural parameters that can be tuned in the quasiperiodic designing compared with the periodic structures. For example, Fibonacci sequence contains two different building blocks.[2] In this work, we investigate spin-dependent transport in quasiperiodic cascade junctions of FM and SC, where FM and SC are arranged in the Fibonacci sequence.

Consider a Fibonacci cascade junction (FCJ) of FM and SC, where FM and SC are arranged in the Fibonacci sequence. Two building blocks, A and B, are arranged according to the rule $S_{j+1}=\{S_j, S_{j-1}\}$, where $S_1=\{A\}$ and $S_2=\{AB\}$. In our system, each building block is constructed by one FM layer and one SC layer. The FM layers in both A and B blocks have the same thickness d_f, but the SC layer have the thicknesses d_s^A in the A block and d_s^B in the B block. Suppose that spin along the x-axis in a quasi-one-dimensional waveguide constructed as FCJ of FM and SC. Electrons are confined in the y-direction by an asymmetric quantum well in the SC, where the Rashba spin-orbit coupling exists. The magnetization of FM layers is chosen along the z-direction, which is parallel to the interface. Then the Hamiltonians in the FM and SC regions can be written as

$$\hat{H}_f = \frac{1}{2}\hat{p}_x \frac{1}{m_f^*}\hat{p}_x + \frac{1}{2}\Delta\sigma_Z \tag{1}$$

and

$$\hat{H}_s = \frac{1}{2}\hat{p}_x \frac{1}{m_s^*}\hat{p}_x + \frac{1}{2\hbar}\sigma_Z[\hat{p}_x\alpha_R + \alpha_R\hat{p}_x] + \delta E, \tag{2}$$

respectively. Here, m_f^* and m_s^* are the effective masses of electrons in the FM and SC regions, respectively. Δ is the exchange splitting energy in the FM, σ_z denotes the spin Pauli matrices, α_R is the spin-orbit Rashba parameter, and δE is the conduction-band mismatch between SC and FM.

Because the Hamiltonians shown in Eqs. (1) and (2) are spin diagonal, the electronic eigenstates in the whole system have the form of $|\Psi_\uparrow\rangle=[\psi_\uparrow(x), 0]$ and $|\Psi_\downarrow\rangle=[0, \psi_\downarrow(x)]$. In the lth FM/SC cell, the eigenstate in the FM region has the form

$$\psi_\sigma^{f,l} = A_\sigma^l e^{ik_{F\sigma}^{f,l}(x-x_l)} + B_\sigma^l e^{-ik_{F\sigma}^{f,l}(x-x_l)}, \tag{3}$$

and the eigenstate in the SC region is

[a)]Electronic mail: rlzhang@nju.edu.cn.
[b)]Electronic mail: rwpeng@nju.edu.cn.

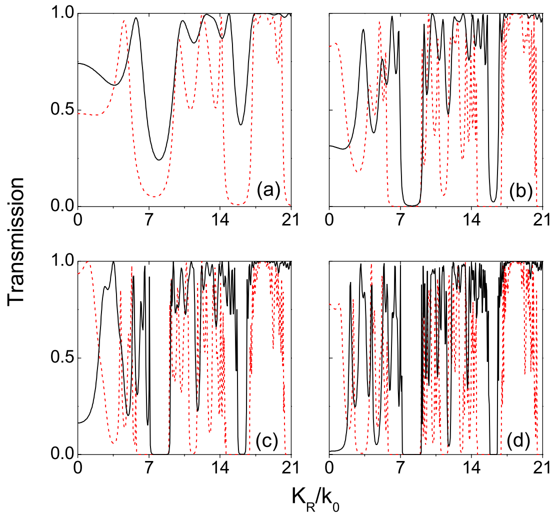

FIG. 1. (Color online) The spin-dependent transmission coefficients as a function of the Rashba spin-orbit wave vector in the FCJs with different numbers of cells (N): (a) $N=5$, (b) $N=13$, (c) $N=21$, and (d) $N=34$. The solid line and the dash one correspond to spin-down and spin-up electrons, respectively. We assume that $m_s^*=0.036m_e$, $m_f^*=m_e$, and m_e is the free electron mass. The Fermi wave vectors for spin-up and spin-down electrons are set as $k_{F\uparrow}=0.44\times10^8\ \text{cm}^{-1}$ and $k_{F\downarrow}=1.05\times10^8\ \text{cm}^{-1}$, respectively. The conduction-band mismatch between the SC and FM is $\delta E=2.4$ eV. All these parameters are reasonable for Fe- and InAs-based heterostructures. The thicknesses of FM and SC have been set as $d_f=1$ nm and $d_s^A=0.1\ \mu$m, $d_s^B=0.08\ \mu$m, respectively. And $k_0=1\times10^5\ \text{cm}^{-1}$, which can be reached in experiments.

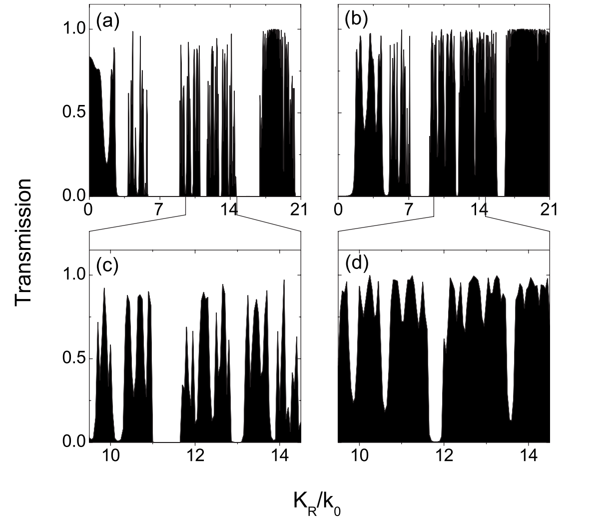

FIG. 2. (a) Transmission coefficient against the Rashba spin-orbit wave vector for the spin-up electron in the FCJ with $N=55$. (b) Transmission spectra of the spin-down electron in the FCJ with $N=55$. [(c) and (d)] The enlargement of the central regions of (a) and (b), respectively.

$$\psi_\sigma^{s,l} = C_\sigma^l e^{ik_{F,+\sigma}^s(x-x_l-d_f/2-d_s/2)} + D_\sigma^l e^{-ik_{F,-\sigma}^s(x-x_l-d_f/2-d_s/2)}, \quad (4)$$

where d_s equals d_s^A (or d_s^B) in the A block (or in the B block), x_l is the central position of the FM layer in the lth cell along the x-axis, $\sigma=\uparrow,\downarrow$ indicates the spin state of the split band, $k_{F\sigma}^{f,l}$ is the Fermi wave vector in the lth FM layer, $k_{F,\pm\sigma}^s$ is the Fermi wave vector in the SC layer, and $+\sigma$ (or $-\sigma$) indicates the same (or opposite) spin state with σ. By using the continuous conditions, the coefficients of A_l, B_l and A_{l+1}, B_{l+1} in two adjacent FM layers are related by a transfer matrix M_l. And the whole system is represented by a product matrix M,relating the incident and reflection waves to the transmission wave. The transmission coefficient of the electron with the spin state σ through the whole FCJ can be described by

$$T_\sigma = \left(\frac{k_{F\sigma}^{f,N+1}}{k_{F\sigma}^{f,1}}\right)\left|\frac{1}{M_{22}}\right|^2. \quad (5)$$

M_{22} is an element of M. Once the spin-dependent transmission coefficients T_σ is achieved, the spin polarization P and conductance G can be expressed as $P=(T_\uparrow-T_\downarrow)/(T_\uparrow+T_\downarrow)$ and $G=(e^2/h)(T_\uparrow+T_\downarrow)$, respectively. Besides, the charge density in FM and SC regions of the lth cell is determined by $|\psi_\sigma^{f,l}(x)|^2$ and $|\psi_\sigma^{s,l}(x)|^2$, respectively.

Based on Eq. (5), the spin-dependent transmission coefficient can be calculated as a function of the Rashba spin-orbit wave vector in the FCJs. It is shown that in Fig. 1, there is no total reflection when the number of cells (N) is small in the FCJ, although there exist some regions of minimum transmission. When N becomes larger, the minima in transmission become extended gradually into the bandgap, where the transmission is blocked. Generally, with increasing cell number of FCJ, more and more transmission zones diminish gradually, and some of them approach zero transmission. In this way, a distinct bandgap structure is realized in the FCJ. It should be noted that spin-up and spin-down electrons possess different bandgap structures against the Rashba spin-orbit wave vector [as shown in Figs. 1(a)–1(d)]. Therefore, a spin-dependent bandgap structure is realized in the FCJs by increasing the cell number. Furthermore, multiple resonant transmissions for spin-up or spin-down electrons can be observed within the bandgap due to the quasiperiodicity of the FCJs. Thus the spin-dependent bandgap structure and the spin-dependent resonant transmission in the bandgap can be obtained when the cell number increases.

The transmission spectra in FCJs also present some other interesting features, such as self-similarity. Figures 2(a) and 2(b) illustrate the transmission coefficients against Rashba spin-orbit wave vectors for spin-up and spin-down electrons, respectively. Here the cell number is set as $N=55$. It is shown that the spin-dependent bandgap structure has the hierarchical characteristic. Figures 2(c) and 2(d) are the enlargement of the central regions of Figs. 2(a) and 2(b), respectively. Obviously, transmission bands and gaps almost correspond to the bands and gaps of the FCJ in the rational approximation. Therefore, the spin-dependent bandgap structure presents good self-similarity. The hierarchical characteristic and self-similarity of the spin-dependent bandgap structure in the FCJ are quite similar to those in the optical and electronic transmission spectra.[4] A similar spin-dependent band structure may be found in other nonperiodic cascade junctions of FM and SC, such as in the Thue–Morse structure.

In order to understand the behavior of spin-up and spin-down electrons clearly, the charge-density distributions in the FCJ has been studied. Figure 3 shows the charge-density distributions in the FCJ of S_8 ($N=34$) with different Rashba spin-orbit wave vectors. As shown in Fig. 1(d), the transmission coefficients of spin-up and spin-down electrons are dif-

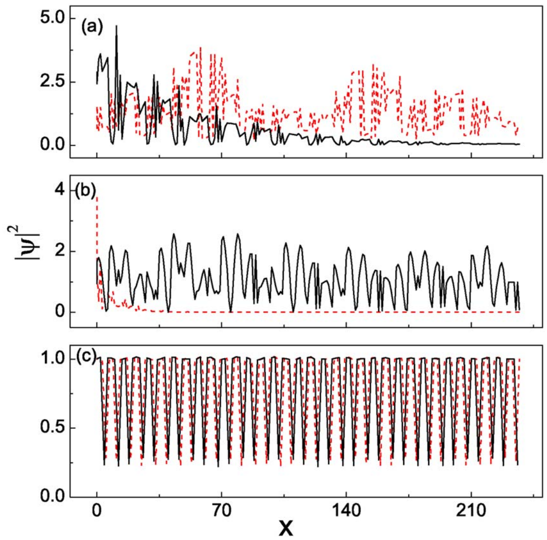

FIG. 3. (Color online) The charge-density distribution in the FCJ of S_8 ($N=34$) with different Rashba spin-orbit wave vectors: (a) $K_R=11.80k_0$, and the transmission coefficients are $T_\uparrow=0.926\,665\,87$ and $T_\downarrow=0.043\,491\,815$. (b) $K_R=14.80k_0$, and the transmission coefficients are $T_\uparrow=6.841\,840\,9\times10^{-11}$ and $T_\downarrow=0.988\,246\,53$. (c) $K_R=18.35k_0$, and the transmission coefficients are $T_\uparrow=0.999\,974\,08$ and $T_\downarrow=0.988\,246\,53$. The solid line and the dash one correspond to spin-down and spin-up electrons, respectively.

ferent at some wave vectors in the FCJ of S_8. It is shown in Figs. 3(a)–3(c) the charge-density distributions of spin-up and spin-down electrons have different behaviors. At the wave vector of $K_R=11.80k_0$, the charge-density distribution of the spin-up electron oscillates quickly with a slowly oscillating envelope, which shows an almost extended state. However the charge-density distribution of the spin-down electron oscillates with a monotonically decreasing envelope, which exhibits a character of the localized state [as shown in Fig. 3(a)]. In other words, the spin-up electron can propagate through the whole system, while the spin-down electron cannot propagate in the system. Figure 3(b) shows the cases of extended state for the spin-down electron and localized state for the spin-up electron. In Fig. 3(c), we give an example of the extended states for both spin-up and spin-down electrons at $K_R=18.35k_0$, which clearly show a periodic distribution of the charge density. In this case, both spin-up and spin-down electrons can propagate through the FCJ of S_8. Therefore, spin filtering can be realized by varying the Rashba spin-orbit wave vector with a gate voltage in the FCJ.

It is interesting to study the spin polarization and total electrical conductance in the FCJs. As shown in Figs. 4(a)–4(d), spin polarization can be changed alternatively from positive to negative when the Rashba spin-orbit wave vector is varied. At some wave vectors, the absolute value of the spin polarization can be changed rapidly from 0 to 1 or from 1 to 0, which originates from the difference in bandgap structures between spin-up and spin-down electrons in the FCJ. Furthermore, high spin polarization has been observed, and the spin polarization has been reversed around resonant wave vectors due to the fact that the resonant transmissions are spin dependent. By increasing the cell number of N, the absolute value of spin polarization gradually increases at the resonant wave vector [as shown in Figs. 4(a)–4(d)]. On the

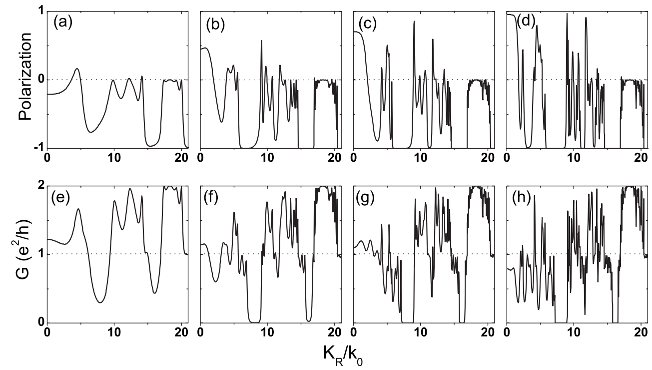

FIG. 4. The spin polarization (P) and conductance (G) against the Rashba spin-orbit wave vector in the FCJs with different cell numbers (N). Spin polarization: (a) $N=5$, (b) $N=13$, (c) $N=21$, and (d) $N=34$. Electrical conductance: (e) $N=5$, (f) $N=13$, (g) $N=21$, and (h) $N=34$.

other hand, the different bandgap structures of the spin-up and spin-down electrons have effects on the electrical conductance in the FCJs. As shown in Figs. 4(e)–4(h), there exist steplike structures within the bandgap in the FCJ. The electrical conductance at the wave vector of the step region is about e^2/h, which comes mainly from one kind of spin electrons. While the electrical conductance is about $2e^2/h$ at the regions where the resonant wave vectors of spin-up and spin-down electrons overlap. These features may provide a unique way to design spin filters and spin switches.

It should be mentioned that in a real system, there usually exists the fluctuation of the layer widths, which definitely reduces the polarization of the FCJs. However, if the fluctuation of the layer widths is less than 4%, the polarization effect can be kept in the FCJ with $N=13$.

This work was supported by grants from the NSFC (Grant Nos. 10625417, 50672035, and 10874068), the MOST of China (Grant Nos. 2004CB619005 and 2006CB921804), and partly by the ME of China and also the Jiangsu Province (Grant Nos. NCET-05-0440 and BK2008012).

[1]D. Shechtman, I. Blech, D. Gratias, and J. W. Cahn, Phys. Rev. Lett. **53**, 1951 (1984).
[2]R. Merlin, K. Bajema, R. Clarke, F.-Y. Juang, and P. K. Bhattacharya, Phys. Rev. Lett. **55**, 1768 (1985).
[3]J. Todd, R. Merlin, R. Clarke, K. M. Mohanty, and J. D. Axe, Phys. Rev. Lett. **57**, 1157 (1986).
[4]M. Kohmoto, B. Sutherland, and K. Iguchi, Phys. Rev. Lett. **58**, 2436 (1987); R. W. Peng, M. Wang, A. Hu, S. S. Jiang, G. J. Jin, and D. Feng, Phys. Rev. B **57**, 1544 (1998); G. J. Jin, Z. D. Wang, A. Hu, and S. S. Jiang, J. Appl. Phys. **85**, 1597 (1999).
[5]R. W. Peng, X. Q. Huang, F. Qiu, M. Wang, A. Hu, S. S. Jiang, and M. Mazzer, Appl. Phys. Lett. **80**, 3063 (2002); R. W. Peng, M. Mazzer, and K. W. J. Barnham, *ibid.* **83**, 770 (2003).
[6]S. Datta and B. Das, Appl. Phys. Lett. **56**, 665 (1990).
[7]E. I. Rashba, Phys. Rev. B **62**, R16267 (2000); G. Kirczenow, *ibid.* **63**, 054422 (2001); S. F. Alvarado, Phys. Rev. Lett. **75**, 513 (1995); H. Ohno, Science **281**, 951 (1998).
[8]A. T. Hanbicki, O. M. J. van't Erve, R. Magno, G. Kioseoglou, C. H. Li, B. T. Jonker, G. Itskos, R. Mallory, M. Yasar, and A. Petrou, Appl. Phys. Lett. **82**, 4092 (2003); X. Jiang, R. Wang, R. M. Shelby, R. M. Macfarlane, S. R. Bank, J. S. Harris, and S. S. P. Parkin, Phys. Rev. Lett. **94**, 056601 (2005).
[9]F. Mireles and G. Kirczenow, Phys. Rev. B **66**, 214415 (2002).
[10]Y. Guo, X.-W. Yu, and Y.-X. Li, J. Appl. Phys. **98**, 053902 (2005); K. M. Jiang, Z. M. Zheng, B. Wang, and D. Y. Xing, Appl. Phys. Lett. **89**, 012105 (2006).